IEEE Access
Multidisciplinary | Rapid Review | Open Access Journal

Received June 19, 2018, accepted July 16, 2018, date of publication July 25, 2018, date of current version August 20, 2018.

Digital Object Identifier 10.1109/ACCESS.2018.2859592

Numerical Analysis of Influences From Internal Waves on Electromagnetic Scattering From Sea Surface

TAO SONG[1], CHUANGMING TONG[1], AND LILI CONG[2]
Air Defense and Anti-missile College, Air Force Engineering University, Xi'an 710051, China
Information and Navigation College, Air Force Engineering University, Xi'an 710051, China

Corresponding author: Tao Song (chinataoguo1990@163.com)

This work was supported by the National Natural Science Foundation of China under Grant 61372033.

ABSTRACT A reliable approach based on a two-scale facet-based model and a wave-number spectrum balance equation is presented to analyze the influences from internal waves on electromagnetic scattering from a particular electrically large sea surface. It could be applied to synthetic aperture radar imagery simulation and calculating the scattering coefficients of sea surface with foam, oil film, and ship wake because local scattering coefficients are available. The facet-based model is derived from the Fucks' first-order small perturbation method function, and then, we give the formula of scattering from arbitrary slope facet taking the two-scale model into consideration. The propagation model of internal waves is established by the Korteweg–de Vries equation, and the mechanism of modulation from internal waves to sea surface spectrum is elucidated on the basis of wave-number spectrum balance equation. Moreover, several examples and theoretical analysis are carried out to investigate the impact of internal waves on scattering characteristics under different parameters. Advisable radar parameters to observe internal waves are suggested based on the results of simulations.

INDEX TERMS Electromagnetic scattering, facet-based model, internal wave, sea surface.

I. INTRODUCTION

Investigation on electromagnetic (EM) scattering from maritime scene is of great value in both civil and military applications, such as, maritime environment monitoring, clutter rejection in target detection, etc. Extensive endeavors have been devoted to explore the scattering characteristic of sea surface. As numerical methods are too tricky and time-consuming for general applications, particularly for electrically large maritime scene, analytical methods have received more and more attention in view of their clear physical interpretation, high efficiency, and relative accuracy. Kirchhoff approximation (KA) [1], small perturbation method (SPM) [2] and small slope approximation (SSA) [3] have been widely used in the sea surface scattering simulation. Crombie [4] firstly discovered the Bragg resonant phenomena that waves resonant with EM waves dominate in the echo. And then two-scale theory has been always a famous approach since it was presented in the 1970s [5]. Further, the modified two-scale method was presented and validated with better accuracy [6]. However, the above are statistic approaches that obtain an average of the scattering coefficients under different conditions without a particular sea height map. Meanwhile, nothing is said about local information which is desirable in Synthetic Aperture Radar (SAR) imagery simulation of maritime scene, especially the one with internal waves. Zhang *et al.* [7] and Chen *et al.* [8] came up with a slope-determined facet model which could give both the total and local scattering contributions in mono- or bistatic system. It could be handily applied to SAR imagery simulation.

Internal waves are the interior fluctuations which occur in the layer with steady density. Due to the density difference of layers, small disturbance gives rise to huge waves inside the sea. They play an important role in the mass and energy transfer of ocean. What is more, SAR has been used to observe the internal waves since the 1970s, which discovers that the grain of SAR images varies when internal waves travel through. It indicates that internal waves have an effect on the EM scattering coefficients of ocean. Similarly, internal waves would make a difference on sea remote sensing, parametric inversion and target detection, etc. Therefore, it is of significance to explore the effect of internal waves on sea EM scattering, on which the research is scanty.

Although satellite-based SAR works at microwave band and the penetrability is weak, it could observe the internal waves travelling at dozens of meters depth under sea. In order to investigate the characteristics of SAR images with internal waves travelling through, some experiments on sea remote sensing have been performed [9]–[11]. Depending on these experimental data, some scholars have investigated the imaging mechanism of internal waves. Alpers [12] delivered a paper on Nature in 1985 which explained the mechanism of internal waves imaging. He pointed out that the propagation process of internal wave altered the interior field of sea, and then modulated the surface capillary waves. As a result, amplitude-gathering and amplitude-diffusion effects took place on surface capillary waves. According to Bragg scattering mechanism [13], the scattering coefficients of sea surface would also be changed, which leads to dark-light stripes on SAR images. This conclusion is still widely accepted by scholars in correlated field now. Some endeavors have been devoted to explore the effect of internal waves on sea EM scattering in theory. Zheng *et al.* [14] gave the variation curves of scattering coefficients when internal waves occurred based on Korteweg-de Vries (KdV) equation, spectrum balance equation and Bragg scattering theory. Although this research mainly aimed at the inversion of internal wave parameters, it referred to the analysis of the effect of internal waves on sea EM scattering coefficients. On the basis of this work, Brandt *et al.* [15] introduced the two-scale model to improve the EM scattering model. This model took the fluctuation of large scale waves into consideration and matches well with reality. Li [16] studied on the process of internal wave SAR imaging systematically and analyzed the effect of internal wave parameters, radar parameters and sea parameters on scattering coefficients. Similarly, Yue *et al.* [17] analyzed the effect of different radar frequencies, different polarizations, different incident angles and wind angles on scattering coefficients aiming at finding out the optimal radar parameters to detect internal waves. All the researches mentioned above referred to the effect of internal waves on sea surface scattering coefficients, whereas their aims were not at building reasonable scattering model to analyze the scattering characteristics of internal waves systematically and thoroughly. And the local information was missing which is necessary in SAR imagery simulation.

In this work, the propagation model of internal wave is established based on KdV equation and the modulation of capillary waves spectrum is derived on the basis of wave-number spectrum balance equation. Moreover, a two-scale facet-based model (TSFBM) derived from Fuks' first order small perturbation method function [18], [19] is proposed to calculate the scattering contribution from individual sea surface facets with internal waves taken into consideration. Finally, several simulation results are given to investigate the effect of internal waves on EM scattering characteristics under different conditions.

II. MODEL DESCRIPTION AND FORMULATION

A. PROPAGATION MODEL OF INTERNAL WAVES

The propagation process of internal waves in flow mechanics can be expressed by KdV Equation [20].

$$\frac{\partial \eta}{\partial t} + (C_0 + \alpha\eta + \alpha_1\eta^2)\frac{\partial \eta}{\partial x} + \beta\frac{\partial^3 \eta}{\partial x^3} = 0 \tag{1}$$

where η is the vertical displacement of internal wave; t denotes time; x stands for the spatial location; C_0 indicates the velocity of linear wave.

For simplification, it is assumed that the sea is composed of two layers and one (upper layer) is above the thermocline, the other one (lower layer) is beneath the thermocline. The depths of upper layer and lower layer are h_1 and h_2, respectively. Then the total depth of sea is $h = h_1 + h_2$. In the two-layer scheme, α, α_1, and β can be expressed as

$$\alpha = \frac{3C_0(h_1 - h_2)}{2h_1h_2} \tag{2}$$

$$\alpha_1 = \frac{3C_0}{h_1^2h_2^2}\left[\frac{7}{8}(h_2 - h_1)^2 - (h_2^2 - h_1h_2 + h_1^2)\right] \tag{3}$$

$$\beta = \frac{C_0h_1h_2}{6} \tag{4}$$

where the velocity of linear wave can be calculated by

$$C_0 = \sqrt{\frac{g\Delta\rho}{\rho}\frac{h_1h_2}{h_1 + h_2}} \tag{5}$$

where $\Delta\rho = \rho_2 - \rho_1$ indicates the density difference in sea water between lower layer and upper layer; ρ is the mean density and $\Delta\rho/\rho$ is the normalized density difference.

Substituting (2)-(5) into (1) to solve the KdV equation, we can get the stable state salutation of solitary wave [16].

$$\eta(x, t) = \pm\eta_0 sech^2\left[\frac{x - C_0't}{l}\right] \tag{6}$$

where η_0 is the maximum amplitude of internal wave; if $h_1 < h_2$, then $\alpha < 0$, (6) is minus and the internal wave is concave; if $h_1 > h_2$, then $\alpha > 0$, (6) is positive and the internal wave is convex; C_0' is the phase velocity and l indicates the half-wave width of internal wave which can be expressed as

$$C_0' = C_0 + \alpha\eta_0/3 = C_0\left[1 + \frac{\eta_0(h_2 - h_1)}{2h_2h_1}\right] \tag{7}$$

$$l = \frac{2h_1h_2}{\sqrt{3\eta_0\,|h_2 - h_1|}} \tag{8}$$

The current velocity of surface layer along x direction induced by internal wave can be expressed by

$$U_x = \pm\frac{C_0\eta_0}{h_1}\sec h^2\left[\frac{x - C_0't}{l}\right] \tag{9}$$

where the sign is positive when the internal wave is concave whereas negative when the internal wave is convex.

The schematic plot of solitary internal wave is shown in Fig. 1 taking the concave internal wave for example.

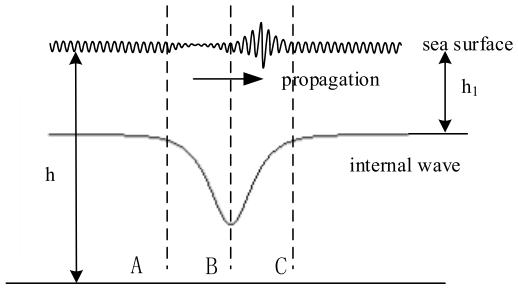

FIGURE 1. Schematic plot of solitary internal wave.

B. SPECTRUM MODULATION BY INTERNAL WAVES

The micro scale characteristics of sea surface related to microwave remote sensing should be the ultra-short waves with several decimeters, centimeters and millimeters wavelength. The fluctuation is slight steep to the above ultra-short waves, so the growing process of surface wave spectrum in wave number space could be expressed by wave-number spectrum balance equation as follows:

$$\frac{\partial \varphi(\boldsymbol{k})}{\partial t} + (c_g + U)\nabla\varphi(\boldsymbol{k}) = S_{in}(\boldsymbol{k}) + S_{nl}(\boldsymbol{k}) + S_{ds}(\boldsymbol{k}) + S_{cu}(\boldsymbol{k}) \quad (10)$$

where $\varphi(\boldsymbol{k})$ indicates the sea spectrum; $\mathbf{k}$ is sea wave-number vector; the four terms on the right side of the equation stand for source function of wind importation, source function of wave-wave interaction, source function of dissipation and source function of wave-current interaction, respectively. The influences from internal waves on sea surface spectrum mainly contribute to the source function of wave-current interaction. As a result, when studying on internal waves, we can simplify (10) as

$$\left[\frac{\partial}{\partial t} + (c_g + U)\frac{\partial}{\partial x}\right]\Delta\varphi(\boldsymbol{k}) = S_{cu}(\boldsymbol{k}) \quad (11)$$

where $\Delta\varphi(\boldsymbol{k})$ indicates the variation value of sea surface spectrum induced by internal waves. Referring to [14], we can express the source function of wave-current interaction as

$$S_{cu} = -\left(S_{\alpha\beta}\frac{\partial U_\beta}{\partial x_\alpha}\right)\varphi(\boldsymbol{k}) \quad (12)$$

Sea water could be regarded as deep water for high band of sea spectrum, so $S_{\alpha\beta}\frac{\partial U_\beta}{\partial x_\alpha}$ could be written as

$$S_{\alpha\beta}\frac{\partial U_\beta}{\partial x_\alpha} = \left[\frac{\partial u}{\partial x}\cos^2\phi + \frac{\partial v}{\partial y}\sin^2\phi + \left(\frac{\partial u}{\partial y} + \frac{\partial v}{\partial x}\right)\cos\phi\sin\phi\right]\Big/2 \quad (13)$$

where u and v are velocity components of large scale flow field; $\emptyset$ is the included angle between the directions of radar vision and internal wave propagation. Substituting (9) into (13), we can get

$$S_{\alpha\beta}\frac{\partial U_\beta}{\partial x_\alpha} = \pm\left(\frac{C_0\cos^2\phi}{h_1 l}\right)\eta_0 \cdot \sec h^2\left(\frac{x - C_0' t}{l}\right) th\left(\frac{x - C_0' t}{l}\right) \quad (14)$$

where the sign is positive when the internal wave is convex whereas negative when the internal wave is concave. Substituting (14) into (11), we can calculate the modulated quantity of sea spectrum induced by internal wave [14].

$$\Delta\varphi(\boldsymbol{k}) = \pm m_3^{-1}\omega^{-1}k^{-4}\eta_0\left(\frac{C_0\cos^2\phi}{h_1 l}\right) \cdot \sec h^2\left(\frac{x - C_0' t}{l}\right) th\left(\frac{x - C_0' t}{l}\right) \quad (15)$$

where the sign is positive when the internal wave is concave whereas negative when the internal wave is convex.

C. TWO-SCALE FACET-BASED MODEL

In view of high efficiency, the large sea surface is generated by the linear filter method which can be combined with inverse fast Fourier transform (IFFT). Firstly, we transfer white noise to frequency domain by Fourier transform, and then filter it with a sea spectrum. In this way, the sea surface fluctuation $\eta(\boldsymbol{\rho}, t)$ can be expressed by

$$\eta(\boldsymbol{\rho}, t) = \sum_{\mathbf{k}} \tilde{\eta}_L(\mathbf{k}, t)e^{i\mathbf{k}\cdot\boldsymbol{\rho}} \quad (16)$$

where $\boldsymbol{\rho} = (x_g, y_g)$ is position vector, and the plural amplitude $\tilde{\eta}_L(\mathbf{k}, t)$ in frequency domain can be written as

$$\tilde{\eta}_L(\mathbf{k}, t) = \chi(\mathbf{k})\pi\sqrt{2\varphi(\mathbf{k})/A}e^{-i\omega(\mathbf{k})t} + \chi^*(-\mathbf{k})\pi\sqrt{2\varphi(-\mathbf{k})/A}e^{-i\omega(-\mathbf{k})t} \quad (17)$$

where χ is a plural Gauss variable whose mean value equals to 0 and standard deviation equals to 1; A indicates the area of sea surface; t is time factor.

Sea surface can be seen as two-scale model that small scale waves are superimposed on the large scale waves. We generate sea surface with ELH spectrum [21] because it involves both long and short wind driven waves. Then the sea surface is decomposed into facets with different slopes. In the case of moderate incident angles and smooth sea surface, interactions and multiple scattering among facets could be negligible. Then we can get the total scattering coefficient by summing up contributions from all the facets. To study on the contributions of internal wave to the sea surface EM scattering, the scattering model should be able to calculate the local scattering. Therefore, an adequate formula for scattering from arbitrary slope facet is needed to derive.

As shown in Fig. 2, assuming that a unit incident plane wave E_i irradiates the microscopic rough surface in xoz plane, we can calculate the scattering coefficient according to the first order small perturbation method presented by Fuks and Voronovich [18] and Fuks [19],

$$\sigma_{pq}^0(\mathbf{k}_i, \mathbf{k}_s) = \pi k^4 |\varepsilon - 1|^2 \left|F_{pq}\right|^2 \varphi(\mathbf{q}_l) \quad (18)$$

where $\mathbf{k}_i$ is a unit vector directed from the transmitter, $\mathbf{k}_s$ is a unit vector directed to the receiver; k indicates the EM wave number; ε denotes the relative permittivity of the dielectric surface, $\varphi(\mathbf{q}_l)$ is the spatial power spectrum of microscopic rough surface; $\mathbf{q}_l$ is the projection vector of $\mathbf{q} = (\mathbf{k}_s - \mathbf{k}_i)$ on

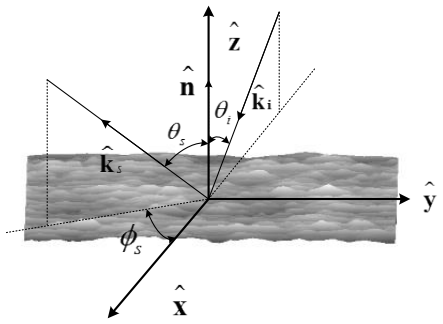

FIGURE 2. Geometry of microscopic rough scattering surface.

the plane $z = 0$, $p, q = h, v$ stand for the polarization directions of scattering and incident waves, respectively, F_{pq} represents the polarization factor which can be calculated by

$$F_{vv} = \frac{1}{\varepsilon}\left[1 + R_v(\theta_i)\right]\left[1 + R_v(\theta_s)\right]\sin\theta_i \sin\theta_s - \left[1 - R_v(\theta_i)\right]\left[1 - R_v(\theta_s)\right]\cos\theta_i \cos\theta_s \cos\phi_s \tag{19}$$

$$F_{vh} = \left[1 - R_v(\theta_i)\right]\left[1 + R_h(\theta_s)\right]\cos\theta_i \sin\varphi_s \tag{20}$$

$$F_{hv} = \left[1 + R_h(\theta_i)\right]\left[1 - R_v(\theta_s)\right]\cos\theta_s \sin\varphi_s \tag{21}$$

$$F_{hh} = \left[1 + R_h(\theta_i)\right]\left[1 + R_h(\theta_s)\right]\cos\varphi_s \tag{22}$$

where R_v and R_h are the Fresnel reflection coefficients with different polarizations, θ_i, θ_s, $\emptyset_s$ are the incident angle, scattering angle and scattering azimuth angle, respectively.

Next, we derive the computing formula of scattering from arbitrary slope facet.

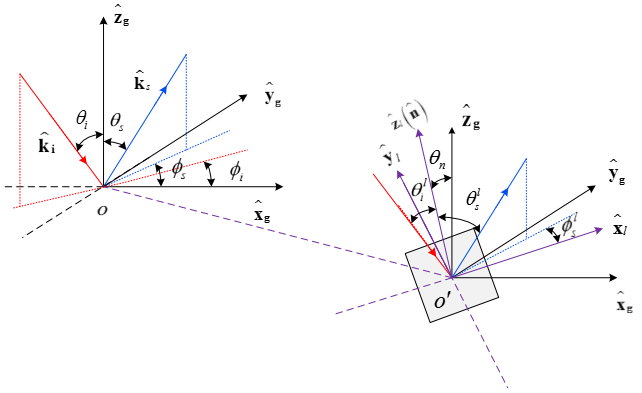

FIGURE 3. Geometry of local coordinate and global coordinate.

As shown in Fig. 3, $\{\mathbf{x_g}, \mathbf{y_g}, \mathbf{z_g}\}$ is the global coordinate and the local coordinate is created at the point o' of facet as follows:

$$\mathbf{z}_l = \mathbf{n} \tag{23}$$

$$\mathbf{y}_l = \mathbf{n} \times \mathbf{k}_i / |\mathbf{n} \times \mathbf{k}_i| \tag{24}$$

$$\mathbf{x}_l = \mathbf{y}_l \times \mathbf{z}_l \tag{25}$$

where $\mathbf{n} = \left(-Z_x \mathbf{x_g} - Z_y \mathbf{y_g} - \mathbf{z_g}\right)/\sqrt{1 + Z_x^2 + Z_y^2}$ indicates the normal vector of the facet; $(\theta_i, \theta_s, \emptyset_i, \emptyset_s)$ and $\left(\theta_i^l, \theta_s^l, \emptyset_i^l, \emptyset_s^l\right)$ are the global and local angles of incidence and scattering direction in different coordinates.

Referring to (18), we can get the scattering coefficient of arbitrary slope rough facet

$$\sigma_{PQ}^{facet}(\mathbf{k}_i, \mathbf{k}_s) = \pi k^4 |\varepsilon - 1|^2 \left|\widetilde{F}_{PQ}\right|^2 \varphi(\mathbf{q}_l) \tag{26}$$

where $\tilde{F}_{PQ}$ is defined as the polarization factor in global coordinate which can be obtained from the following relation:

$$\begin{pmatrix} \widetilde{F}_{VV} & \widetilde{F}_{VH} \\ \widetilde{F}_{HV} & \widetilde{F}_{HH} \end{pmatrix} = \begin{pmatrix} \mathbf{V}_s \cdot \mathbf{v}_s & \mathbf{H}_s \cdot \mathbf{v_s} \\ \mathbf{V}_s \cdot \mathbf{h}_s & \mathbf{H}_s \cdot \mathbf{h}_s \end{pmatrix} \begin{pmatrix} F_{vv} & F_{vh} \\ F_{hv} & F_{hh} \end{pmatrix} \times \begin{pmatrix} \mathbf{V}_i \cdot \mathbf{v}_i & \mathbf{V}_i \cdot \mathbf{h}_i \\ \mathbf{H}_i \cdot \mathbf{v}_i & \mathbf{H}_i \cdot \mathbf{h}_i \end{pmatrix} \tag{27}$$

where $(\mathbf{H}_i, \mathbf{V}_i, \mathbf{H}_s, \mathbf{V}_s)$ and $(\mathbf{h}_i, \mathbf{v}_i, \mathbf{h}_s, \mathbf{v}_s)$ are the unit polarization vectors in global and local coordinates, respectively.

According to the Bragg resonance hypothesis, both the Bragg waves spreading along and against the radar sight direction contribute to the radar receiver, thus above two-scale facet-based model (TSFBM) can be rewritten as

$$\sigma_{PQ}^{facet}(\mathbf{k}_i, \mathbf{k}_s) = \pi k^4 |\varepsilon - 1|^2 \left|\widetilde{F}_{PQ}\right|^2 \varphi_{capi}(\mathbf{q}_l) \tag{28}$$

where $\varphi_{capi}(\mathbf{q}_l) = \frac{1}{2}\left[\varphi_E^{capi}(-\mathbf{q}_l) + \varphi_E^{capi}(\mathbf{q}_l)\right]$ is the Bragg waves component; φ_E^{capi} is the small-scale capillary ripple part of one-sided ELH spectrum.

Thus cut-off wave number k_{cut} is introduced to divide ELH spectrum into small-scale capillary ripple part φ_E^{capi} and large-scale gravity wave part φ_E^{grav}.

$$\varphi_E^{grav}(\mathbf{k}) = \begin{cases} 0, & |\mathbf{k}| \geq \pi/6 \\ \varphi_E(\mathbf{k}), & |\mathbf{k}| \leq \pi/6 \end{cases} \tag{29}$$

$$\varphi_E^{capi}(\mathbf{k}) = \begin{cases} \varphi_E(\mathbf{k}), & |\mathbf{k}| \geq \pi/6 \\ 0, & |\mathbf{k}| \leq \pi/6 \end{cases} \tag{30}$$

where $\varphi_E(\mathbf{k})$ is the two-dimensional ELH spectrum and k_{cut} here equals to $\pi/6$.

When the internal waves occur, sea spectrum should be modulated with $\varphi = \varphi_{capi} + \Delta\varphi$. So the scattering coefficient from sea surface facet with internal wave should be calculated by

$$\sigma_{PQ}^{\prime facet}(\mathbf{k}_i, \mathbf{k}_s) = \pi k^4 |\varepsilon - 1|^2 \left|\widetilde{F}_{PQ}\right|^2 \left[\varphi_{capi}(\mathbf{q}_l) + \Delta\varphi(\mathbf{q}_l)\right] \tag{31}$$

Assumed that the lengths of the two-dimensional simulation sea surface sample in x and y directions are L_x and L_y, respectively. The area is $A = L_x L_y$, the numbers of discrete points are M and N, and the distances between two adjacent points are Δx and Δy. Then, according to (31), we can get the total scattering coefficient by summing up the contributions from all of the facets

$$\sigma_{PQ}^{\prime total}(\mathbf{k}_i, \mathbf{k}_s) = \frac{1}{A}\sum_{m=1}^{M}\sum_{n=1}^{N}\left[\sigma_{PQ,mn}^{\prime facet}(\mathbf{k}_i, \mathbf{k}_s)\,\Delta x \Delta y\right] \tag{32}$$

wherein $\sigma_{PQ,mn}^{\prime facet}(\mathbf{k}_i, \mathbf{k}_s)$ is the normalized Bragg scattering coefficient of the number mn facet.

III. NUMERICAL RESULTS AND ANALYSIS

At present, investigations on internal waves are mainly by the SAR remote sensing, so all simulations and investigation in this paper have been realized in the case of monostatic configuration with parameters which SAR always works at. Furthermore, monostatic configuration could also reflect evidently the influence of internal waves on scattering coefficients in spatial domain.

A. INFLUENCES FROM INTERNAL WAVES ON SCATTERING COEFFICIENT

According to the calculation approach above, we give the EM scattering coefficients distribution (HH polarization) of sea surface with and without internal waves in Fig. 4. The computation platform is a personal computer with an Intel 3.2 GHz CPU, 16GB RAM. The calculation time in this simulation is about 102 seconds, which includes the generation of sea surface and the calculation of scattering coefficients.

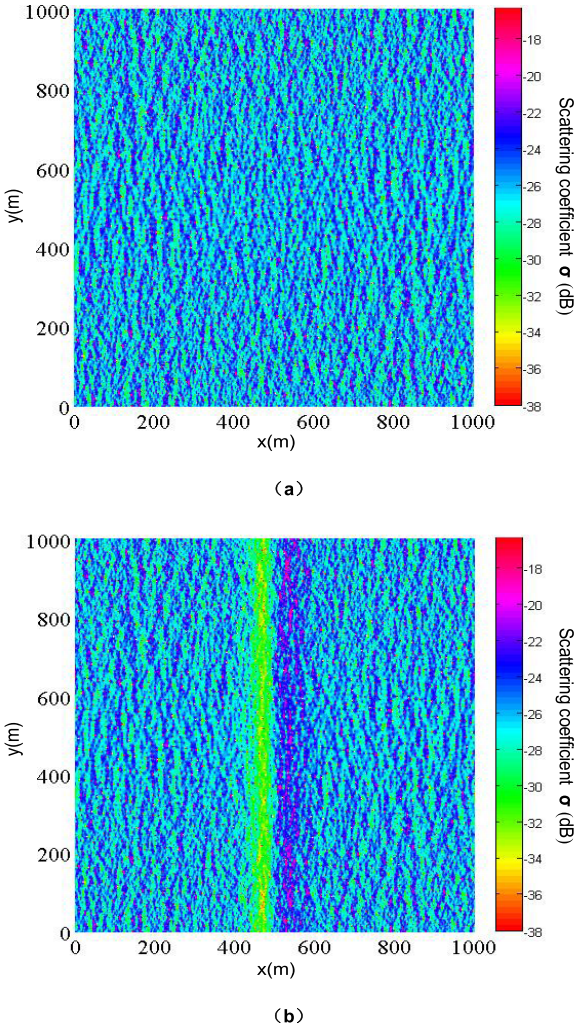

FIGURE 4. Backscattering coefficients distributions of the sea surface with and without internal waves: (a) without internal waves, (b) with internal waves.

Parameters in the simulation are in order as follows: *the SAR remote sensing always works at X-band (10 GHz) and moderate angles, so we set the frequency and incident angle in this simulation are 10.0 GHz and* 40°, *respectively; on the other hand, the scattering coefficients calculated by equation (18) are persuasive and with better accuracy when the incident angle is* 40°; *the azimuth angle of incidence is set as* 0° *for the reason of simplification and better observation;* the angle of wind direction $\emptyset_w$ is defined as the included angle of wind direction and $\hat{x}_g$ axis, here $\emptyset_w = 0°$, the wind speed at 10 m above the mean sea level is selected by $u_{10} = 5.0$ m/s, the relative permittivity calculated by Debye model is $\varepsilon = (56.12, 37.42)$, the numbers of sea surface discrete points are $M = N = 1000$, the distances between two adjacent points are $\Delta x = \Delta y = 1.0\ m$, the depth of upper layer is $h_1 = 15\ m$, the depth of lower layer is $h_2 = 40\ m$, the maximum amplitude of internal wave is $\eta_0 = 10\ m$, and the normalized density difference in sea water between lower and upper layer is $\Delta\rho/\rho = 3.0 \times 10^{-3}$. As the internal wave model given in Section 2 is directionless, we assume that the internal wave travels along $\mathbf{x_g}$ axis and is invariable along $\mathbf{y_g}$ for better observation of the influences of internal waves.

As shown in Fig. 4, the scattering coefficients distributions could reflect the fluctuation of large scale wave both with and without internal wave. What is more, when internal wave, which is concave here, occurs, the scattering coefficient dwindles at the *A*-*B* part in Fig. 1 because the roughness of surface wave diminishes when the amplitude of internal wave decreases. Accordingly, at the B-C part where the amplitude of internal wave increases, scattering coefficient increases by reason of the surface wave becoming rougher. As a result, dark-bright stripe comes into being on the scattering coefficients distribution of sea surface which is in accord with the experimental data in [9].

B. INFLUENCES FROM INTERNAL WAVES UNDER DIFFERENT PARAMETERS

For better investigation on influences from internal waves, we define $\Delta\sigma$ (dB) as the difference of scattering coefficients which can be expressed as

$$\Delta\sigma = 10\log_{10}\sigma_{PQ}^{tfacet}(\mathbf{k}_i, \mathbf{k}_s) - 10\log_{10}\sigma_{PQ}^{facet}(\mathbf{k}_i, \mathbf{k}_s) \tag{33}$$

where $\sigma_{PQ}^{tfacet}(\mathbf{k}_i, \mathbf{k}_s)$ is the scattering coefficient of sea surface facet with internal wave and $\sigma_{PQ}^{facet}(\mathbf{k}_i, \mathbf{k}_s)$ is the scattering coefficient of sea surface facet without internal wave. $\Delta\sigma$ can also be called as modulation depth of internal wave. And only variations along $\mathbf{x_g}$ axis are given for the sake of visualized observation.

Fig. 5 gives the regularity for change of $\Delta\sigma$ under different internal wave parameters. Only results of HH polarization are given here because those of VV polarization are similar. It is necessary to explain that the curve is not smooth because we adopt the two-scale model and the modulation of large scale wave makes the scattering coefficients undulant.

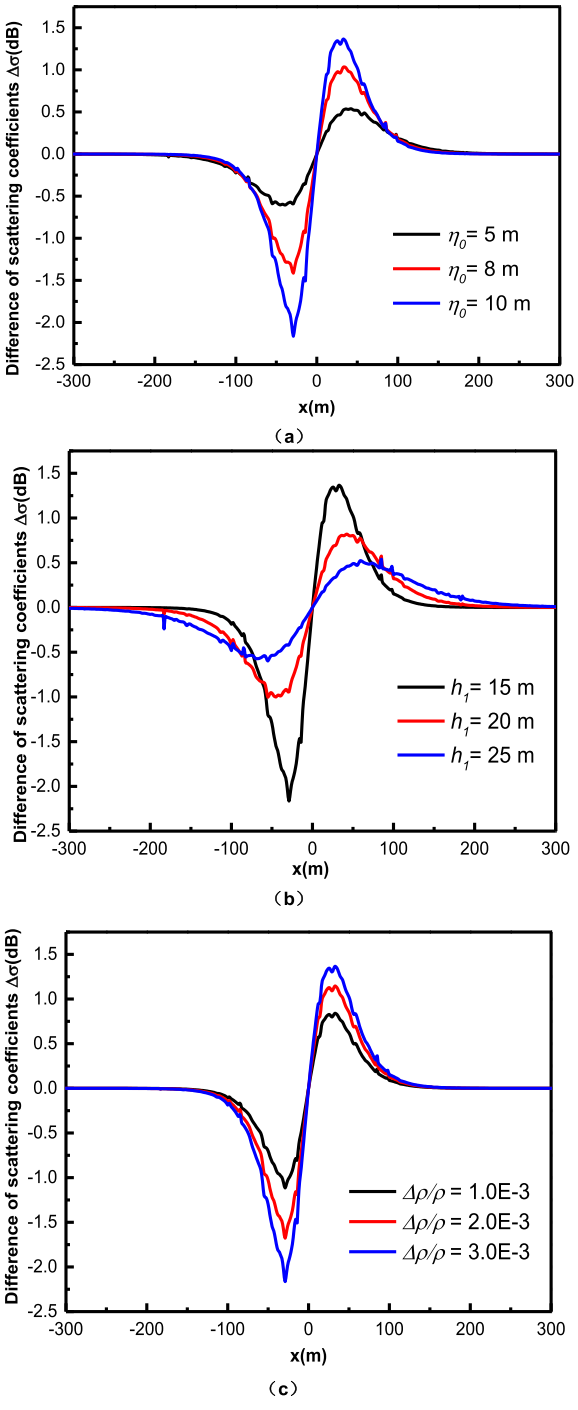

FIGURE 5. Impact of different internal wave parameters on $\Delta\sigma$: (a) maximum amplitude, (b) upper layer depth, (c) normalized density difference.

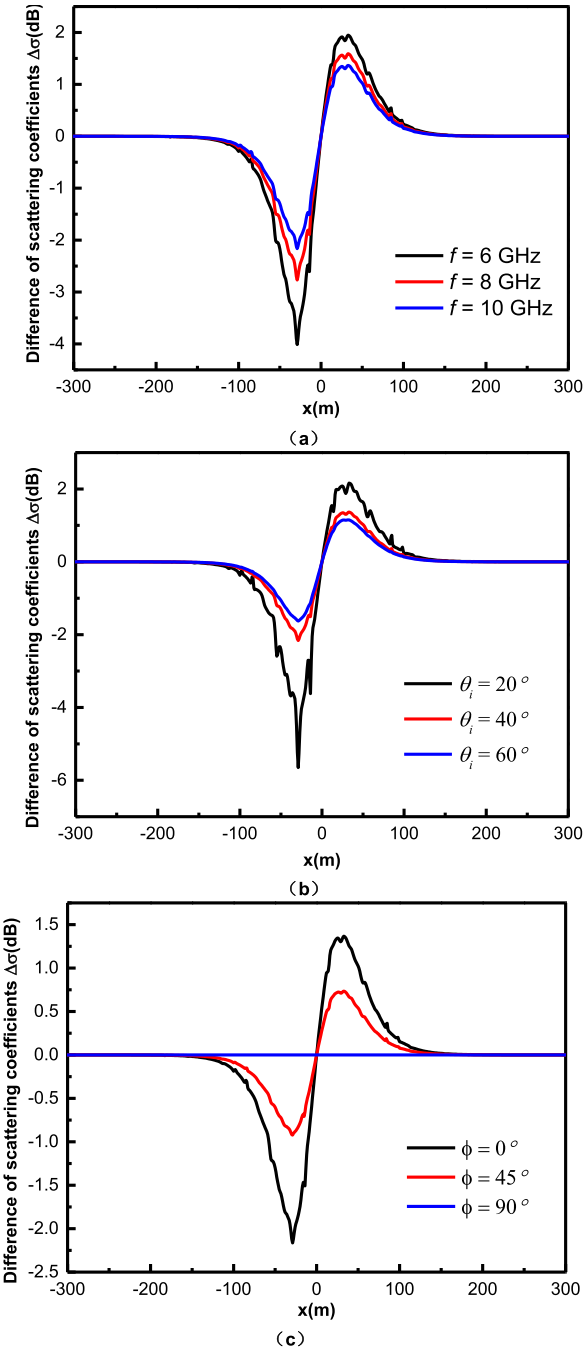

FIGURE 6. Impact of different radar parameters on $\Delta\sigma$: (a) frequency, (b) incident angle, (c) direction of radar vision.

The parameters which are variable are given on figures and the else are the same with above ones.

Fig. 5(a) compares the results of $\Delta\sigma$ with different maximum amplitudes. As we can see, the variation of $\Delta\sigma$ becomes more intense when the maximum amplitude increases, and the impact of internal wave is more remarkable. It is due to that the modulation of surface wave spectrum becomes larger as the maximum amplitude increases. The impact of upper layer depth on $\Delta\sigma$ is shown in Fig. 5(b), and the fluctuation becomes more intense when upper layer depth becomes smaller. The reason is that when the upper layer depth becomes smaller, the disturbance caused by internal wave is easier to spread to the sea surface through wave-current interaction. The impact of normalized density difference $(\Delta\rho/\rho)$ on $\Delta\sigma$ is shown in Fig. 5(c). It determines that the variation of $\Delta\sigma$ becomes more intense when the

normalized density difference increases, because it is the very density difference that generates the internal waves. When disturbance occurs, the density difference makes it grow up and break the steady state of sea water to generate the internal waves. Therefore, the internal wave becomes more intense when the normalized density becomes larger, and the modulation to surface wave spectrum is larger too.

The regularities for change of $\Delta\sigma$ under different radar parameters are shown in Fig. 6. Fig. 6(a) compares the results of $\Delta\sigma$ with different incident wave frequencies and shows that the smaller the frequency is, the more remarkable the impact of internal wave is. Fig. 6(b) gives the results of different incident angles. It indicates that within two-scale model mechanism, the impact of internal wave is more remarkable when the incident angle is smaller. Fig. 6(c) compares the results with different directions of radar vision. When the direction of radar vision parallels to direction of internal wave propagation ($\emptyset = 0°$), the variation of $\Delta\sigma$ is maximum. When the direction of radar vision is normal to the propagation direction of internal wave ($\emptyset = 90°$), $\Delta\sigma$ will equal to zero. The result also explains the reason why it is difficult to observe the internal wave on SAR images which travels parallel to the flight direction of satellites. Above all, the advisable radar parameters in Bragg mechanism to observe internal waves are small frequency, small incident angle and radar visions parallel to direction of internal wave propagation.

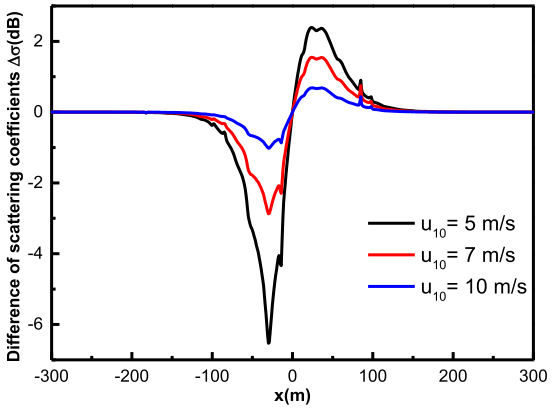

FIGURE 7. Impact of different wind speeds on $\Delta\sigma$.

Fig. 7 gives the regularity for change of $\Delta\sigma$ with different wind speeds. As clearly shown, the impact of internal wave is more unnoticeable when the wind speed grows up. It is on the ground that when the wind speed grows up, the sea surface is rougher and the diffuse scattering increases. The modulation action of internal waves to sea surface would be drowned by strong clutter.

It is necessary to illustrate that the results of simulations in this paper are hard to be validated by measured data directly. The reason is that the related experiment data are always SAR images, and the measured internals in fact are always multiple configurations which are hard to simulate for unprofessional fluid mechanics researchers. Secondly, gamma in SAR images can reflect the variation of scattering coefficients, but the value of scattering coefficients cannot be obtained. So we cannot compare the simulation results with the experimental ones. Furthermore, in view of the time-varying character of sea surface, it is impossible to measure the scattering coefficients difference of the same sea surface with and without internal waves. Even so, the tendency and law of simulations results obtained by the proposed model match well with the experimental data and can explain well the phenomenon in fact, which verifies the validity and accuracy of the proposed model.

IV. CONCLUSION

In this paper, a reliable approach based on TSFBM is developed for the analysis of influences from internal waves on EM scattering from a particular electrically large sea surface, which is of significance in sea remote sensing, parametric inversion and target detection, etc. Both the total and local scattering coefficients could be handily calculated based on this proposed model. So it could be applied to SAR imagery simulation and calculating scattering coefficients of sea surface with foams, oil film, and ship wake. Additionally, the mechanism of modulation from internal waves to sea surface spectrum and scattering coefficients are analyzed. Moreover, the impacts of different parameters on modulation effect of internal waves are analyzed and the advisable radar parameters to observe internal waves are proposed.

REFERENCES

[1] D. Holliday, "Resolution of a controversy surrounding the Kirchhoff approach and the small perturbation method in rough surface scattering theory," *IEEE Trans. Antennas Propag.*, vol. AP-35, no. 1, pp. 120–122, Jan. 1987.

[2] F. Bass, I. Fuks, A. Kalmykov, I. Ostrovsky, and A. Rosenberg, "Very high frequency radiowave scattering by a disturbed sea surface part I: Scattering from a slightly disturbed boundary," *IEEE Trans. Antennas Propag.*, vol. AP-16, no. 5, pp. 554–559, Sep. 1968.

[3] A. Voronovich, "Small-slope approximation for electromagnetic wave scattering at a rough interface of two dielectric half-spaces," *Wave Random Media*, vol. 4, no. 3, pp. 337–367, 1994.

[4] D. Crombie, "Doppler spectrum of sea echo at 13.56 Mc./s," *Nature*, vol. 175, pp. 681–682, Apr. 1955.

[5] F. G. Bass and I. M. Fuks, *Wave Scattering From Statistically Rough Surfaces*. Oxford, U.K.: Pergamon, 1979, pp. 418–442.

[6] Z.-S. Wu, J.-P. Zhang, L.-X. Guo, and P. Zhou, "An improved two-scale model with volume scattering for the dynamic ocean surface," *Prog. Electromagn. Res.*, vol. 89, pp. 39–56, Jan. 2009.

[7] M. Zhang, H. Chen, and H.-C. Yin, "Facet-based investigation on EM scattering from electrically large sea surface with two-scale profiles: Theoretical model," *IEEE Trans. Geosci. Remote Sens.*, vol. 49, no. 6, pp. 1947–1975, Jun. 2011.

[8] H. Chen, M. Zhang, Y.-W. Zhao, and W. Luo, "An efficient slope-deterministic facet model for SAR imagery simulation of marine scene," *IEEE Trans. Antennas Propag.*, vol. 58, no. 11, pp. 3751–3756, Nov. 2010.

[9] B. A. Hughes and J. F. R. Gower, "SAR imagery and surface truth comparisons of internal waves in Georgia Strait, British Columbia, Canada," *J. Geophys. Res., Oceans*, vol. 88, no. C3, pp. 1809–1824, 1979.

[10] B. A. Hughes and T. W. Dawson, "Joint Canada-US Ocean wave investigation project: An overview of the Georgia Strait Experiment," *J. Geophys. Res., Oceans*, vol. 93, no. C10, pp. 12219–12234, 1988.

[11] R. F. Gasparovic and V. S. Etkin, "An overview of the joint US/Russia internal wave remote sensing experiment," in *Proc. IGARSS*, vol. 2, Aug. 1994, pp. 741–743.

[12] W. Alpers, "Theory of radar imaging of internal waves," *Nature*, vol. 314, pp. 245–247, Mar. 1985.
[13] J. C. West, "Correlation of Bragg scattering from the sea surface at different polarizations," *Waves Random Complex Media*, vol. 15, no. 3, pp. 345–403, 2005.
[14] Q.-A. Zheng, Y. Yuan, V. Klemas, and X.-H. Yan, "Theoretical expression for an ocean internal soliton synthetic aperture radar image and determination of the soliton characteristic half width," *J. Geophys. Res., Oceans*, vol. 106, no. C12, pp. 31415–31423, 2001.
[15] P. Brandt, R. Romeiser, and A. Rubino, "On the dependence of radar signatures of oceanic internal solitary waves on wind conditions and internal wave parameters," in *Proc. IGARSS*, vol. 3, Jul. 1998, pp. 1662–1664.
[16] H.-Y. Li, "Studying ocean internal waves with SAR," M.S. thesis, Mar. Environ. College, Ocean Univ. China, Qingdao, China, 2004.
[17] Q. Yue, J. Chong, Y. Wu, and M. Zhu, "Simulation studies of internal waves in SAR images under different SAR and wind field conditions," *IEEE Trans. Geosci. Remote Sens.*, vol. 49, no. 5, pp. 1734–1743, May 2011.
[18] I. M. Fuks and A. G. Voronovich, "Wave diffraction by rough interfaces in an arbitrary plane-layered medium," *Wave Random Media*, vol. 10, no. 2, pp. 253–272, 2000.
[19] I. M. Fuks, "Wave diffraction by a rough boundary of an arbitrary plane-layered medium," *IEEE Trans. Antennas Propag.*, vol. 49, no. 4, pp. 630–639, Apr. 2001.
[20] A. K. Liu, Y. S. Chang, M.-K. Hsu, and N. K. Liang, "Evolution of nonlinear internal waves in the East and South China Seas," *J. Geophys. Res., Oceans*, vol. 103, no. C4, pp. 7995–8008, 1998.
[21] T. Elfouhaily, B. Chapron, K. Katsaros, and D. Vandemark, "A unified directional spectrum for long and short wind-driven waves," *J. Geophys. Res., Oceans*, vol. 102, no. C7, pp. 15781–15796, 1997.

TAO SONG was born in Zaozhuang, Shandong, China, in 1990. He received the B.S. degree in electromagnetic wave propagation and antenna and the M.S. degree in electromagnetic field and microwave technology from Air Force Engineering University, Xi'an, China, in 2013 and 2016, respectively, where he is currently pursuing the Ph.D. degree in electronics science and technology. His research interests include computational electromagnetics and wave scattering from rough surface.

CHUANGMING TONG has more than 20 years of experience in teaching and research. He was a Visiting Scientist Post-Doctoral Fellow with Southeast University, Nanjing, China. He is currently a Professor with the Department of Electronics and Communication Engineering, Air and Missile Defense College, Air Force Engineering University. His research interests include microwave remote sensing, electromagnetic waves, polarimetric and interferometric applications of microwave data, numerical modeling, and ground penetrating radar through wall imaging and stealth technology. He has received various fellowships and awards from national and international bodies.

LILI CONG was born in Weihai, Shandong, China, in 1991. She received the B.S. and M.S. degrees from Air Force Engineering University, CPLA, Xi'an, China, in 2013 and 2015, respectively, where she is currently pursuing the Ph.D. degree in electromagnetic field and microwave technology with the Information and Navigation Institute. She has authored or co-authored over 10 technical journal articles and conference papers. Her main research interests include electromagnetic metamaterials and their antenna applications and wideband RCS reduction of antenna array.